Author's Accepted Manuscript

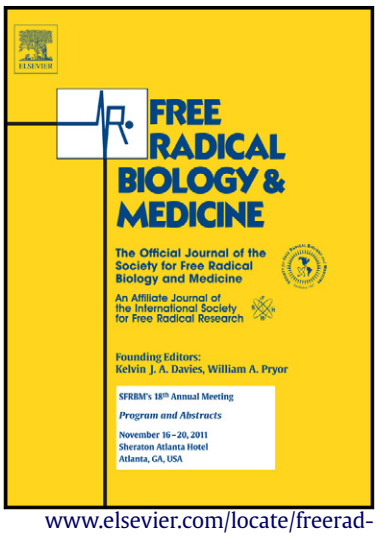

www.elsevier.com/locate/freerad-biomed

Cardiac mitochondrial biogenesis in endotoxemia is not accompanied by mitochondrial function recovery

Virginia Vanasco, Trinidad Saez, Natalia D. Magnani, Leonardo Pereyra, Timoteo Marchini, Alejandra Corach, María Inés Vaccaro, Daniel Corach, Pablo Evelson, Silvia Alvarez

PII: S0891-5849(14)00399-2
DOI: http://dx.doi.org/10.1016/j.freeradbiomed.2014.08.009
Reference: FRB12117

To appear in: *Free Radical Biology and Medicine*

Received date: 15 April 2014
Revised date: 10 July 2014
Accepted date: 20 August 2014

Cite this article as: Virginia Vanasco, Trinidad Saez, Natalia D. Magnani, Leonardo Pereyra, Timoteo Marchini, Alejandra Corach, María Inés Vaccaro, Daniel Corach, Pablo Evelson, Silvia Alvarez, Cardiac mitochondrial biogenesis in endotoxemia is not accompanied by mitochondrial function recovery, *Free Radical Biology and Medicine,* http://dx.doi.org/10.1016/j.freeradbiomed.2014.08.009

This is a PDF file of an unedited manuscript that has been accepted for publication. As a service to our customers we are providing this early version of the manuscript. The manuscript will undergo copyediting, typesetting, and review of the resulting galley proof before it is published in its final citable form. Please note that during the production process errors may be discovered which could affect the content, and all legal disclaimers that apply to the journal pertain.

ACCEPTED MANUSCRIPT

Cardiac mitochondrial biogenesis in endotoxemia is not accompanied by mitochondrial function recovery

Virginia Vanasco [1], Trinidad Saez [2], Natalia D. Magnani [1], Leonardo Pereyra [1], Timoteo Marchini [1], Alejandra Corach [3], María Inés Vaccaro[1], Daniel Corach [3], Pablo Evelson [1] and Silvia Alvarez [1]

[1] Institute of Biochemistry and Molecular Medicine, School of Pharmacy and Biochemistry, University of Buenos Aires-CONICET, Junín 956, C1113AAD Buenos Aires, Argentina.
[2] Institute of Cellular Biology and Neuroscience, School of Medicine, University of Buenos Aires-CONICET, Paraguay 2155, C1121ABG Buenos Aires, Argentina.
[3] Servicio de Huellas Digitales Genéticas, School of Pharmacy and Biochemistry, University of Buenos Aires-CONICET, Junín 956, C1113AAD Buenos Aires, Argentina.

Accepted manuscript

Running title: Cardiac mitochondrial biogenesis in endotoxemia

Corresponding author:
Silvia Alvarez, PhD
Institute of Biochemistry and Molecular Medicine (UBA-CONICET)
School of Pharmacy and Biochemistry
University of Buenos Aires
Junín 956, C1113AAD Buenos Aires, Argentina.
e-mail: salvarez@ffyb.uba.ar
phone: +5411-4508-3646 ext 105

ACCEPTED MANUSCRIPT

ABSTRACT

Mitochondrial biogenesis emerges as a compensatory mechanism involved in the recovery process in endotoxemia and sepsis. The aim of this work was to analyze the time course of cardiac mitochondrial biogenesis process occurring during endotoxemia, with emphasis in the quantitative analysis of mitochondrial function. Female Sprague-Dawley rats (45 days old) were ip injected with LPS (10 mg/kg). Measurements were performed at 0-24h after LPS administration. PGC-1α and mtTFA expression for biogenesis, and p62 and LC3 expression for autophagy, were analyzed by western blot; mitochondrial DNA levels by qPCR, and mitochondrial morphology by transmission electron microscopy. Mitochondrial function was evaluated as oxygen consumption and respiratory chain complexes activity. PGC-1α and mtTFA expression resulted significantly increased in every time-point analyzed, and mitochondrial mass was observed increased by 20% ($p<0.05$) at 24h. p62 expression was found significantly decreased in a time-dependent manner. LC3-II expression was observed significantly increased at all-time points analyzed. Ultrastructurally, mitochondria displayed several abnormalities (internal vesicles, cristae disruption, and swelling) at 6 and 18h. Structures compatible with fusion/fission processes were observed at 24 h. Significant decrease in state 3 respiration was observed in every time-point analyzed (LPS 6h: 20%, $p<0.05$). Mitochondrial complex I activity was found decreased by 30% in LPS-treated animals at 6 and 24h. Complex II and complex IV showed decreased activity only at 24h. The present results show that partial restoration of cardiac mitochondrial architecture is not accompanied by improvement of mitochondrial function in acute endotoxemia. The key implication of our study is that cardiac failure due to bioenergetic dysfunction will be overcome by therapeutic interventions aimed to restore cardiac mitochondrial function.

Accepted manuscript

HIGHLIGHTS

Cardiac mitochondrial biogenesis occurs in acute endotoxemia.
Cardiac mitochondrial function is not fully recovered during biogenesis.
Therapeutic interventions should be targeted to prevent bioenergetic dysfunction.

KEYWORDS

endotoxemia, LPS, O_2 metabolism, mitochondrial biogenesis, mitochondrial function, rat heart

ACCEPTED MANUSCRIPT

ABBREVIATIONS

eNOS	endothelial nitric oxide synthase
EPR	electron spin resonance
LC3	microtubule.associated protein 1 light chain 3
LPS	lipopolisaccharide
mtDNA	mitochondrial DNA
mtTFA	mitochondrial transcription factor A
MM	mitochondrial membranes
NO-Hb	NO-hemoglobin
PGC1α	peroxisome proliferator activated receptor-coactivator α
RCR	respiratory control ratio
ROS	reactive O_2 species

Accepted manuscript

ACCEPTED MANUSCRIPT

INTRODUCTION

Sepsis and endotoxemia are described as a paradigm of acute whole body inflammation, characterized by massive increases of nitric oxide (NO) and inflammatory cytokines in biological fluids, systemic damage in the vascular endothelium, and impaired tissue and whole body respiration despite adequate O_2 supply [1]. Without timely and effective therapeutic intervention, this scenario evolves to multiple organ failure (MOF) and ultimately to death mainly by heart failure [2]. Cardiac sequelae due to systemic inflammation include reversible/irreversible damage to cardiomyocytes, such as impairment of intracellular calcium homeostasis, alterations of excitation/contraction coupling, and enhanced programmed cell death (apoptosis) [3].

There is current awareness about the central role of mitochondrial dysfunction in the development of organ failure in this syndrome [4-6]. Mitochondria provide energy to the cell through the synthesis of ATP by F_o-F_1 ATP synthase. Consequently, a deficient ATP production may result in bioenergetic dysfunction and cardiac failure.

Previous results from our laboratory have shown heart mitochondrial bioenergetic dysfunction with decreased O_2 uptake and ATP production in endotoxemia [7]. Taking this into account, strategies to preserve (as the beneficial effects of α-lipoic acid, previously shown by our laboratory [8]) or restore mitochondrial function could limit cardiac mitochondrial impairment and bioenergetic failure as well as help to prevent organ dysfunction in endotoxemia.

In this scenario, mitochondrial biogenesis emerges as a compensatory mechanism that requires nuclear and mitochondrial genomic orchestration. Signals that activate mitochondrial biogenesis include: NO and reactive O_2 species (ROS) increased production, and energy deprivation. In line with this observation, we have previously found increased NO, $O_2^{\bullet-}$ and H_2O_2 production in cardiac mitochondria during endotoxemia [7]. Moreover, nitric oxide produced by endothelial nitric oxide synthase (eNOS) has been described to be involved in mitochondrial biogenesis in brown adipocytes through a cGMP-dependent pathway [9]. Changes in intracellular levels of ROS have also been associated with changes in mitochondrial number, mitochondrial DNA (mtDNA) copy number and expression of genes involved in the regulation of respiratory complexes expression [10, 11]. Results obtained by Nisoli et al. using different cell lines, in control conditions, and triggering mitochondrial biogenesis by DETA-NO, showed that this process yield functional mitochondria [12]. Of note, although mitochondrial biogenesis triggered *in vivo* and in

Accepted manuscript

ACCEPTED MANUSCRIPT

different physiopathological conditions indicates increased mass of newly mitochondria, this observation does not necessarily imply that resultant mitochondria are functional. The mechanisms by which mitochondrial energy metabolism and sepsis induced myocardial damage are not fully understood. In this way, mitochondrial biogenesis emerges as a compensatory mechanism involved in putative recovery process.

To our knowledge, no studies have been carried out analyzing mitochondrial function during heart mitochondrial biogenesis in an *in vivo* acute inflammatory model as endotoxemia. The aim of this work was to analyze the time course of cardiac mitochondrial biogenesis process during endotoxemia, with emphasis in the quantitative analysis of mitochondrial function.

MATERIALS AND METHODS

Drugs and chemicals

Lipopolisaccharide (LPS, serotype 026:B6 from *Escherichia coli*), was from Sigma-Aldrich (St. Louis, MO, USA). Other reagents, enzymes and chemicals were of reagent grade and also from Sigma-Aldrich.

Experimental design

Rats (Sprague-Dawley, female, 45 ± 5 days old), from the Animal Facility of the School of Pharmacy and Biochemistry of the University of Buenos Aires were used. The animals were housed under standard conditions of light, temperature and humidity, with unlimited access to water and food (pelleted rodent food). LPS was injected i.p in a single dose of 10 mg/kg body weight. Measurements were performed at different time points (0-24 h) after LPS administration. As control group, animals were handled in parallel and received the same volume of saline solution (vehicle). Animal treatment was carried out in accordance to the guidelines of the 6344/96 regulation of the Argentine National Drug, Food and Medical Technology Administration (ANMAT).

Body temperature

Body temperature was determined by measuring rectal temperature in animals using a digital thermometer (MT-Esatherm Ltd. 8172, Czech Republic) with a 2 mm sensor diameter.

Accepted manuscript

ACCEPTED MANUSCRIPT

NO-hemoglobin (NO-Hb) in blood by electron paramagnetic resonance (EPR)

Rats were anesthetized [ketamine (50 mg/kg) plus xylazine (0.5 mg/kg)], and blood was obtained by cardiac puncture and immediately stored at 77 K (liquid N_2) until analyzed. The EPR spectrum of NO-Hb was determined at 77 K in a Bruker spectrometer ECS 106 (Karlsruhe, Germany) with a ER 4102ST cavity. The parameters of the spectra were as follows: field modulation frequency, 50 kHz; microwave frequency, 9.42; modulation amplitude, 4.75 G; microwave power, 10 mW; time constant, 164 ms; sweep width, 800 gauss; center field, 3300 gauss [13]. The quantification of the spectra was performed by calculating the area under the curve (double integral of the spectrum). The results are expressed in arbitrary units.

Tissue processing for transmission electron microscopy and micrograph analysis

Rats were anesthetized with [ketamine (50 mg/kg) plus xylazine (0.5 mg/kg)], heart was rapidly removed and washed with 0.1 M K_2HPO_4/KH_2PO_4, pH 7.4. Left ventricular myocardium was removed and cut into 1 mm^3 cubes. Tissue sample was fixed with 2.5% glutaraldehyde in 0.1 M K_2HPO_4/KH_2PO_4 (pH 7.4) during 2 h and post-fixed in 1% osmium tetroxide in 0.1 M K_2HPO_4/KH_2PO_4 for 1.5 h at 0°C. Samples were contrasted with 5% uranyl acetate for 2 h at 0°C, dehydrated and embedded in Durcupan resin (Fluka AG, Switzerland) for 72 h at 60°C. Ultrathin sections were cut and observed with a Zeiss EM 109 transmission electron microscope (Oberkochen, Germany). Representative digital images were captured using a CCD GATAN ES1000W camera (California, USA). Random sections were selected for analysis by an electron microscopy technician blinded to the treatments. Using the “point counting grids” methodology [14], mitochondrial density was determined. Damaged mitochondria [15] and mitochondria with swelling were also analyzed. Damaged mitochondrial index included mitochondria with: internal vesicles, cristae and membrane disruption and cleared matrix.

Homogenate preparation

Rats were anesthetized [ketamine (50 mg/kg) plus xylazine (0.5 mg/kg)] and heart was immediately excised and placed in ice-cold isolation buffer (250 mM sucrose, 5 mM Tris/HCl, 2 mM EGTA, 0.25% BSA, 2.5 $MgCl_2$, 0.5 mM ATP pH 7.4). Left ventricle was isolated from heart and the tissue was homogenized in a glass–Teflon homogenizer in 5 ml of isolation buffer plus 2.5 UI/ml type XXIV bacterial proteinase. Homogenates were

Accepted manuscript

ACCEPTED MANUSCRIPT

centrifuged at 8000 g for 10 min to discard the presence of protease. The pellet was resuspended in 4 ml STE buffer (250 mM sucrose, 5 mM Tris/HCl and 2 mM EGTA, pH 7.4), centrifuged at 700 *g* for 10 min to discard nuclei and cell debris, and the sediment was discarded. Supernatant was used for cytochrome oxidase activity, and mitochondria isolation. Protein content was assayed with the Folin reagent using bovine serum albumin as standard [16].

Western blot analysis

Cardiac left ventricle was removed and homogenized in a Bio-Gen pro200 homogenizer (Pro Scientific) in 1 ml of ice-cold western blot buffer (50 mM Hepes, 100 mM NaCl, 1 mM EDTA, 20 mM NaF, 20 mM $Na_4P_2O_7$, $NaVO_3$ 1 mM, 1% Triton x-100, 1% SDS, pH 7.4; plus 1 µg/ml peptatin, 1 µg/ml aprotinin, 1 µg/ml leupeptin and 0.4 mM phenylmethanesulfonyl fluoride). After a 10 min incubation at 2 ºC, the sample was sonicated twice (30 s with 1 min interval), and centrifuged at 800 *g* for 20 min. The supernatant was used for western blot analysis.

Equal amounts of proteins (50 µg) were separated by SDS-PAGE (7.5%, 10% or 12%) and blotted into nitrocellulose films. Non-specific binding was blocked by incubation of the membranes with 5% non-fat dry milk in PBS for 1 h at room temperature. Membranes were probed with 1:500 diluted goat polyclonal antibodies against PGC1 [PGC-1 (K-15): sc-5816; Santa Cruz Biotechnology, Santa Cruz, CA], mtTFA [mtTFA (V-13): sc-30965; Santa Cruz Biotechnology, Santa Cruz, CA], LC3B [LC3B antibody (2775); Cell Signaling Technology, MA], p62 [SQSTM1 (P-15): sc-10117; Santa Cruz Biotechnology, Santa Cruz, CA] or mouse monoclonal anti β-actin [β-actin (C4): sc-47778; Santa Cruz Biotechnology, Santa Cruz, CA]. The nitrocellulose membrane was subsequently incubated with a secondary rabbit anti-goat antibody (Santa Cruz Biotechnology, Santa Cruz, CA), rabbit anti-mouse antibody [(315-035-048) Jackson InmunoResearch, Baltimore Pike, USA] or goat anti-rabbit antibody [(GAR):170-5046; Bio-Rad, CA] conjugated with horseradish peroxidase (dilution 1:10,000 or 1:5,000) and revealed by chemiluminiscence with ECL reagent. Band images were quantified digitally, using SCION image Sofware, and data was expressed as relative to β-actin expression [17].

Accepted manuscript

ACCEPTED MANUSCRIPT

DNA extraction and quantification

DNA was extracted as previously described [18]. Quantification was performed by real-time PCR (StepOne Plus, Life Technologies, Foster City, CA , USA) using two pairs of primers (Table 1) amplifying a single copy region of the genome located on chromosome 3 in the region corresponding to Topoisomerase I gene (Top1), and a mitochondrial genomic region outside the larger deletion corresponding to NADH dehydrogenase I gene (mt- Nd1). All amplicons are 153 bp in length. The reaction was carried out in triplicate for each primer pair used, and for each treatment /control. Mitochondrial DNA comparative quantification was analyzed by the algorithm $2^{-\Delta\Delta Ct}$ method [19].

Mitochondrial isolation and preparation of mitochondrial membranes

The homogenate previously obtained (as in homogenate preparation section) was centrifuged at 8000 *g* for 10 min to precipitate mitochondria [16]. The mitochondrial pellet was washed twice and resuspended in the same isolation buffer; it consisted of mitochondria able to carry out oxidative phosphorylation. Purity of isolated mitochondria was assessed by determining lactate dehydrogenase activity; only mitochondria with less than 5% impurity were used [20]. Mitochondrial membranes (MM) were obtained by freezing and thawing mitochondria three times, homogenizing by passage through a 29G hypodermic needle [20]. Protein content was assayed with the Folin reagent using bovine serum albumin as standard.

Oxygen uptake by mitochondria

A two-channel respirometer for high-resolution respirometry (Hansatech Oxygraph, Hansatech Instruments Ltd, Norfolk, England) was used. Heart mitochondrial respiration was measured in a reaction medium containing 120 mM KCl, 5 mM KH_2PO_4, 1 mM EGTA, 3 mM HEPES, 1 mg/ml BSA, 2 mM malate and 5 mM glutamate, pH 7.2 and 0.3–0.4 mg/ml of fresh heart mitochondria, at 25 °C. In this condition, state 4 respiration rate was measured; 1 mM ADP was added to establish state 3 respiration [21]. Results were expressed as ng-at O/min. mg protein. Respiratory control ratio (RCR) was calculated as the ratio between state 3/state 4 respiration rates. RCR greater than 7 (in control animals) have been routinely observed, characteristic of high mitochondrial integrity. Furthermore, exogenous cytochrome c does not significantly enhance mitochondrial respiration (10%)

Accepted manuscript

ACCEPTED MANUSCRIPT

suggesting minimal damage to the outer mitochondrial membrane during isolation procedures.

Respiratory complexes activity

For the determination of NADH-cytochrome *c* reductase (complex I) activity, 0.02 mg/ml MM were added to 0.1 M K_2HPO_4/KH_2PO_4 (pH 7.4), 25 µM cytochrome c^{3+}, 0.2 mM NADH and 0.5 mM KCN ,and followed spectrophotometrically at 550 nm (ε = 19.6 mM^{-1} cm^{-1}) in a Beckman DU 7400 diode array spectrophotometer at 30°C. Results were expressed as nmol cytochrome c^{2+}/min.mg protein. Succinate cytochrome *c* reductase activity (complex II) was similarly determined and expressed, except that NADH was substituted by 5 mM succinate. Cytochrome oxidase activity (complex IV) was assayed spectrophotometrically at 550 nm by following the oxidation rate of 50 mM cytochrome c^{2+} [22] in 0.1M K_2HPO_4/KH_2PO_4 (pH 7.4), 50 µM cytochrome c^{2+} and 0.02 mg/ml MM or 0.02 mg/ml homogenate. Results were expressed as k´/mg protein.

Mitochondrial ATP production rate

The chemiluminescent assay is based in the luciferine-luciferase reaction; ATP production rate was measured in a reaction medium containing 120 mM KCl, 20 mM Tris–HCl, 1.6 mM EDTA, 0.08% BSA, 8 mM K_2HPO_4/KH_2PO_4, 0.08 mM $MgCl_2$, pH 7.4, 40 µM luciferine, 1 µg/ml luciferase and 30–50 µg of heart mitochondria at 28 °C. 6 mM Malate, 6 mM glutamate, 0.1 mM ADP, and 0.15 mM di(adenosine)pentaphosphate were added to the reaction medium [23]. The measurement was made in a LKB Wallack 1209 Rackbeta liquid scintillation counter. The production of ATP in the presence of 2 µg/ml oligomycin was determined and a calibration curve using ATP as standard (0–20 nmoles) was performed [23]. ATP production rate was expressed as nmol ATP/min. mg protein.

Statistics

Results were expressed as mean values ± SEM and represent the mean of five independent experiments. ANOVA followed by Dunnett test or Bonferroni test was used to analyze differences among experimental groups. Statistical significance was considered at $p < 0.05$.

Accepted manuscript

ACCEPTED MANUSCRIPT

RESULTS

Body temperature and NO-Hb levels

Six hours after LPS injection, animals showed a significant increase in body temperature with respect to control group (control: 37.1 ± 0.2 ºC, $p < 0.05$), while 12 h after LPS injection, the animals showed significant hypothermia ($p < 0.01$) (Fig.1). Fig. 2, panel A shows three typical spectra corresponding to blood NO-Hb signals. Fig.2; panel B shows NO-Hb signal quantification. NO-Hb levels were found increased in endotoxemic animals at every time point analyzed.

Mitochondrial biogenesis time course

A 92 kDa protein was identified by western blot analysis reacting with anti- PGC-1α antibodies in left ventricle homogenate. Its expression was significantly increased at all-time points analyzed after LPS injection, as determined by densitometric quantitation of the bands. Results are shown in Fig. 3, panel A. In addition, levels of mtTFA expression were found significantly increased since 6h of LPS treatment (Fig.3, panel B).

Since cytochrome oxidase is exclusively located in mitochondria (inner membrane), the ratio between its activity in the homogenate and in mitochondrial fractions is a useful tool for analyzing mitochondrial mass [24]. Table 2 shows a significant increase (20%, $p < 0.05$) in this parameter only 24 h after LPS injection.

Figure 4, shows mitochondrial and nuclear DNA quantification. After 18h, mitochondrial DNA levels were observed significantly decreased by 67% compared to control and 6h LPS groups. However, no significant difference was observed at 24h after LPS treatment with respect with control group. This observation suggests a recovery in the amount of mitochondrial DNA at 24 h.

As a first approach to evaluate the occurrence of autophagy, p62 and LC3 expression were analyzed. p62 expression was found significantly increased at 6 h after LPS treatment followed by a time-dependent decrease of the expression (Fig 5 panel A). LC3-II expression was observed significantly increased at all-time points analyzed (Fig 5 panel B).

In order to evaluate morphological changes associated with fusion/fission processes involved in mitochondrial biogenesis, the ultrastructure of left ventricle cardiomyocites was analyzed by transmission electron microscopy. Control rats displayed normal mitochondrial morphology including well-defined double membranes with normal

Accepted manuscript

ACCEPTED MANUSCRIPT

cristae arrangements and preserved morphology and size (Fig. 6, panel A and B). Six and 18 h after LPS administration, mitochondria displayed several abnormalities, such as formation of internal vesicles (Fig. 6, panel C; H and I) loss and/or disruption of cristae (panel D), cleared matrix and swelling (Figure 6, panel F, H and I), and cleared matrix with vacuoles and crests loss (panel C in Fig. 6). Twenty four hours after LPS administration, mitochondria of different sizes and mitochondrial structures compatible with the fission/fusion processes were observed (Fig. 6, panel J and K). However, some cristae disruption and mitochondrial swelling was still observed. Mitochondrial volume density was significantly increased (18%, $p<0.001$) 6h after the treatment; at 18 and 24 h the values showed no significant differences respect to control value (Table 3). The quantification of damaged mitochondria (including swelling, loss and/or disruption of cristae, cleared matrix and internal vesicles) showed increased values (2 to 1.6 times with respect to control value) 6-24 h after the treatment with LPS (Table 3).

Mitochondrial function time course

With the aim of analyzing mitochondrial function, different approaches were used. Oxygen consumption in state 4 (resting or controlled respiration) and in state 3 (active respiration, the maximal physiological rate of O_2 uptake and ATP synthesis), ATP production rates, and the activity of the respiratory chain complexes I, II and IV, were measured. Figure 7 shows a representative measurement of mitochondrial O_2 consumption in control, LPS 6h, LPS 18h and 24h conditions. Significant decreases in state 3 respiration (using malate and glutamate as substrates) were observed after 6 to 24 h of LPS treatment (LPS 6h: 20%, $p<0.05$; Table 4). Using succinate as substrate, a significant decrease was observed only after 24 h of LPS treatment (24 h: 20%, $p<0.05$; Table 4). No significant changes were observed in state 4. Respiratory control ratios (RCR) were observed decreased in treated animals, probably due to decreased state 3 respiration. Complex I activity, shown in Table 5, was found 30% decreased in animals at 6 and 18 h after LPS treatment with respect to the control group (control value: 328 ± 22 nmol/min. mg protein). This decrease was more pronounced (40%, $p < 0.01$) after 24 h of treatment. Complex II and complex IV showed decreased activity (with respect to the control group) only at 24 h after LPS-treatment. Finally, significant decreases (40-60%) were observed in mitochondrial ATP production rates after 6 to 24h of LPS challenge respect the control group (control value: 420 ± 47 nmol ATP/min mg protein, $p<0.05$) (Figure 8).

Accepted manuscript

ACCEPTED MANUSCRIPT

DISCUSSION

Cardiac mitochondrial dysfunction occurring during endotoxemia and sepsis plays a key role in the development of organ damage mainly by decreasing ATP availability and producing increased amounts of reactive oxygen and nitrogen species [7]. However, it has also been proposed that endotoxemia and sepsis might trigger the activation of mitochondrial biogenesis process, which involves a bi-genomic program of nuclear- and mitochondrial-encoded gene regulation that rapidly adjusts mitochondrial mass, functionality and distribution, in order to restore a functional mitochondrial population [25-27]. This process needs proper interplay between nucleus and mitochondria, and coordinated transcription of activating factors. In particular, PGC-1α appears to be the main transcription factor regulating *de novo* synthesis of mitochondrial proteins by inducing the transcription of mtTFA (mitochondrial transcription factor A) [28].

To our knowledge, no studies have been carried out analyzing mitochondrial function during cardiac mitochondrial biogenesis in an acute inflammatory model as endotoxemia at different time points. Because of the complex nature of mitochondria, multiple parameters need to be analyzed in order to ascertain whether mitochondrial biogenesis program is occurring in this pathological context. In this work, we analyzed the time course (0, 6, 12, 18 and 24 h after LPS injection) of heart mitochondrial biogenesis by four different approaches, as follows: a) PGC-1α expression (being one of the key transcription factors involved in early stages of this process) and mtTFA expression (a key activator of mitochondrial DNA transcription and replication) by western blotting; b) mitochondrial mass, analyzed by the relationship between cytochrome oxidase activity in the homogenate and mitochondrial fraction, c) mitochondrial DNA levels by quantitative PCR, and d) mitochondrial morphology by transmission electron microscopy. Of note, mitochondrial function was also analyzed through the determination of O_2 consumption and RCR, activity of the respiratory chain complexes, and mitochondrial ATP production rate.

Increased levels of NO, oxidative stress, and elevated AMP/ATP ratio, among others, have been described as signals inducing mitochondrial biogenesis [29]. In this report, blood NO levels, a marker of the occurrence of the inflammatory process, were observed increased at 6 h after LPS treatment and remained increased during all the other time points assessed. This is a very fast and transient increase in NO production; in acute

Accepted manuscript

ACCEPTED MANUSCRIPT

endotoxemia it has been described that the inflammatory response peak is observed between 6-10 h after LPS challenge [7, 30, 31]. In line with this observation, we previously described that mitochondrial NO production and functional activity of mtNOS were significantly increased at 6h after LPS treatment [7]. The accepted view is that the effect of NO on mitochondrial biogenesis is a general phenomenon; NO effects can be differentially analyzed regarding steady-state levels reached and origin. On the one hand, in basal conditions, it was shown that a moderate NO increase, not only produced by eNOS [9] but provided by NO-donors as N-acetyl penicillamine [12], was able to activate mitochondrial biogenesis in rodent muscle cells and adipocytes. Decreased mitochondrial mass, accompanied with a decrease in O_2 consumption and ATP levels, were observed, in gastrocnemius muscle of eNOS-deficient animals [32]. In pathological models, the scenario is not fully understood and constitutes a challenging question. In inflammatory conditions as endotoxemia, increased NO production is mainly due to iNOS induction [6, 31, 33, 34].

Our laboratory has previously shown that the increase in NO steady state concentration in the heart of endotoxemic animals goes from 22 nM to 28 nM [33]. It is worth to note that in pathological models, increased levels of NO may exert multiple inhibitory actions on mitochondrial function [35, 36]. This observation can be made extensive to tissues with higher O_2 demand and oxidative metabolism, showing that NO effect on mitochondrial biogenesis is a general phenomenon.

PGC-1α expression levels were found increased at 6 h after LPS administration, suggesting the initiation of the mitochondrial biogenesis process. PGC-1α has been identified as a central transcriptional co-activator of nuclear respiratory factor 1 (NRF-1), GA binding protein transcription factor alpha subunit (GABPA) and peroxisome proliferator-activated receptors (PPARs), and is also involved in the physiological integration of mitochondrial biogenesis with oxidative metabolism [37, 38]. In order to analyze downstream signaling pathways of PGC1α, mtTFA expression levels were studied finding its expression significantly increased since 6h of LPS treatment.

Mitochondrial mass, expressed in mg of mitochondrial protein per g of left ventricular myocardium, was observed increased 24 h after the initiation of the endotoxemic process (Table 2), and after the increase in blood NO levels and PGC-1α expression. The analysis of mitochondrial mass through this approach was previously performed in a rat model of ovarian stimulation [24]. In the previously referred table cytochrome oxidase activity is informed per gram of tissue (left ventricle; whole organ

Accepted manuscript

ACCEPTED MANUSCRIPT

activity) and per mg of mitochondrial protein (intrinsic activity in mitochondria). In the first case, although some variations are observed no significant differences were obtained for the different time-points analyzed. In the second case, a slight but significant decrease is observed after 24 h of the treatment. These results may indicate that (for the respiratory chain functionality) intrinsic decrease in complex IV activity is not compensated by the increase in mitochondrial mass observed at 24 hs (activity ratio homogenate/mitochondria). In order to confirm the occurrence of mitochondrial biogenesis, mitochondrial DNA levels were analyzed by qPCR. While there is a significant decrease in mitochondrial DNA levels at 18 h (possibly due to the cleaning of damaged DNA), mitochondrial DNA levels recoveries at 24h are in agreement with the observed increase in mitochondrial mass. Mitochondrial morphology showed disruption and/or loss of mitochondrial inner membrane and outer membrane, mitochondrial swelling and mitochondrial membrane-associated vacuoles at 6, 18 and 24 h after LPS treatment. These changes have been related to the occurrence of oxidative stress [39], and are consistent with the observation of cardiac mitochondrial dysfunction at 6 h after the treatment with LPS, previously published by our laboratory [7]. Mitochondrial volume density was observed significantly increased only at 6h. Although ultrastructural damage was still present after 24 h of treatment with LPS, the occurrence of mitochondrial remodeling processes and a significant diversity in the size were observed.

The process of mitochondrial biogenesis, that enables intermitochondrial cooperation by allowing exchange of membrane and matrix components, might help to restore local depletions and maintain mitochondrial function [40]. However, mitochondrial O_2 consumption in state 3 (with malate and glutamate as respiratory substrates) and ATP production were observed decreased since 6h after treatment with LPS. Moreover, mitochondrial O_2 consumption, RCR and mitochondrial complex I activity did not return to normal values at time points where mitochondrial biogenesis markers were observed significantly increased. It is worth to note that complex II and IV presented a decrease in activity at 24 h, suggesting worsening of mitochondrial function. Although decreased activities of respiratory complexes is mainly attributed to oxidative/nitrosative damage due to increased NO levels, decreased expression levels cannot be ruled out. Previous work of Suliman et al [41] show that after 6 h after LPS challenge PGC-1α levels are observed increased and that after 24 h of an LPS challenge expression levels of Complex I and IV are observed decreased (50% and 30% respectively).

Accepted manuscript

ACCEPTED MANUSCRIPT

In a cell culture model, Nisoli et al. [12] found that induced mitochondrial biogenesis was accompanied by increased O_2 consumption through coupled cellular respiration functionally linked to enhanced ATP production in different cell lines. It is worth noting that in this model, mitochondrial biogenesis was induced in cells having intact and functional mitochondrial population. Oppositely, in our model, mitochondrial biogenesis develops in a scenario characterized by mitochondrial dysfunction, with decreased O_2 consumption and ATP production rate. It is likely therefore that the biogenesis process triggered during this pathological situation is not enough to restore mitochondrial function, ultimately leading to cardiac damage.

Although in this work we elected to study the process of mitochondrial biogenesis as a compensatory mechanism to cope with damaged mitochondria and its relationship to the mitochondrial energetic capacity, the compensatory mechanism that may be activated is complex. The final scenario of this pathology derives from a complex relationship between different processes aimed to cope with decreased energy producing capacity of the organ. These processes mainly include mitochondrial biogenesis, autophagy and cell death.

Consequently, p63 and LC3 expression was analyzed to evaluate the occurrence of autophagy. The early p62 increased expression followed by a time-dependent decrease is in agree with an early activation of its expression by LPS stimulus followed by a degradation phase due to the occurrence of authophagy [42, 43]. LC3-II expression was observed increased at all time-points analyzed, observation that also agrees with the occurrence of this process. Moreover, p62 time-course degradation is consistent with increased autophagy flux after LPS treatment [44]. It was previously shown [45] in a similar model that autophagy is activated prior to mitochondrial biogenesis. It is unclear if autophagy is induced as part of a cellular program leading to apoptosis or as an attempt to removed damaged mitochondria. The occurrence of biogenesis after the activation of mitophagy would reflect a cellular effort to replace damaged mitochondria eliminated by autophagy and, in consequence, restore mitochondrial energy producing capacity. The analysis of the relationships between cell death, mitochondrial biogenesis and autophagy opens a new and vacant area of investigation that emerges as potential target for pharmacological intervention.

To our knowledge, this is the first study that shows that partial restoration of mitochondrial architecture may be not accompanied by improvement of mitochondrial function. The relevance of the observation that mitochondrial biogenesis is not associated

Accepted manuscript

ACCEPTED MANUSCRIPT

with improved cardiac mitochondrial function, consequently non-functional mitochondria, in LPS treated rats may imply that the compensatory mechanism network activated might not be adequate to cope with the damage caused by systemic inflammation. The key implication of our study is that cardiac failure due to bioenergetic dysfunction will be overcome by therapeutic interventions aimed to restore cardiac mitochondrial function.

ACKNOWLEDGEMENTS

The authors are grateful to the Sabrina Troche and Dr. Carlos Bertoli for the helpful assistance with transmission electron microscopy studies.

FUNDING

This work was supported by research from the University of Buenos Aires [grant B107], Agencia Nacional de Promoción Científica y Tecnológica (ANPCYT) [PICT 1574], and Consejo Nacional de Investigaciones Científicas y Técnicas (CONICET) [PIP 0076].

Accepted manuscript

REFERENCES

[1] Szabó, C., Pathophysiological roles of nitric oxide in inflammation. Academic Press ed. 2000, San Diego.

[2] Feuerstein, G.Z. Cardiac RAGE in sepsis: call TOLL free for anti-RAGE. Circ Res. **102** (10): 1153-4; 2008.

[3] Chagnon, F., Metz, C.N., Bucala, R., and Lesur, O. Endotoxin-induced myocardial dysfunction: effects of macrophage migration inhibitory factor neutralization. Circ Res. **96** (10): 1095-102; 2005.

[4] Boveris, A., Alvarez, S., and Navarro, A. The role of mitochondrial nitric oxide synthase in inflammation and septic shock. Free Radic Biol Med. **33** (9): 1186-93; 2002.

[5] Callahan, L.A. and Supinski, G.S. Downregulation of diaphragm electron transport chain and glycolytic enzyme gene expression in sepsis. J Appl Physiol (1985). **99** (3): 1120-6; 2005.

[6] Escames, G., Lopez, L.C., Ortiz, F., Lopez, A., Garcia, J.A., Ros, E., and Acuna-Castroviejo, D. Attenuation of cardiac mitochondrial dysfunction by melatonin in septic mice. FEBS J. **274** (8): 2135-47; 2007.

[7] Vanasco, V., Magnani, N.D., Cimolai, M.C., Valdez, L.B., Evelson, P., Boveris, A., and Alvarez, S. Endotoxemia impairs heart mitochondrial function by decreasing electron transfer, ATP synthesis and ATP content without affecting membrane potential. J Bioenerg Biomembr. **44** (2): 243-52; 2012.

[8] Vanasco, V., Cimolai, M.C., Evelson, P., and Alvarez, S. The oxidative stress and the mitochondrial dysfunction caused by endotoxemia are prevented by alpha-lipoic acid. Free Radic Res. **42** (9): 815-23; 2008.

[9] Nisoli, E., Clementi, E., Paolucci, C., Cozzi, V., Tonello, C., Sciorati, C., Bracale, R., Valerio, A., Francolini, M., Moncada, S., and Carruba, M.O. Mitochondrial biogenesis in mammals: the role of endogenous nitric oxide. Science. **299** (5608): 896-9; 2003.

ACCEPTED MANUSCRIPT

[10] Gadaleta, M.N., Rainaldi, G., Lezza, A.M., Milella, F., Fracasso, F., and Cantatore, P. Mitochondrial DNA copy number and mitochondrial DNA deletion in adult and senescent rats. Mutat Res. **275** (3-6): 181-93; 1992.

[11] Lee, H.C., Yin, P.H., Lu, C.Y., Chi, C.W., and Wei, Y.H. Increase of mitochondria and mitochondrial DNA in response to oxidative stress in human cells. Biochem J. **348 Pt 2**: 425-32; 2000.

[12] Nisoli, E., Falcone, S., Tonello, C., Cozzi, V., Palomba, L., Fiorani, M., Pisconti, A., Brunelli, S., Cardile, A., Francolini, M., Cantoni, O., Carruba, M.O., Moncada, S., and Clementi, E. Mitochondrial biogenesis by NO yields functionally active mitochondria in mammals. Proc Natl Acad Sci U S A. **101** (47): 16507-12; 2004.

[13] Galleano, M., Simontacchi, M., and Puntarulo, S. Nitric oxide and iron: effect of iron overload on nitric oxide production in endotoxemia. Mol Aspects Med. **25** (1-2): 141-54; 2004.

[14] Medeiros, D.M. Assessing mitochondria biogenesis. Methods. **46** (4): 288-94; 2008.

[15] Acehan, D., Vaz, F., Houtkooper, R.H., James, J., Moore, V., Tokunaga, C., Kulik, W., Wansapura, J., Toth, M.J., Strauss, A., and Khuchua, Z. Cardiac and skeletal muscle defects in a mouse model of human Barth syndrome. J Biol Chem. **286** (2): 899-908; 2011.

[16] Mela, L. and Seitz, S. Isolation of mitochondria with emphasis on heart mitochondria from small amounts of tissue. Methods Enzymol. **55**: 39-46; 1979.

[17] Bustamante, J., Bersier, G., Badin, R.A., Cymeryng, C., Parodi, A., and Boveris, A. Sequential NO production by mitochondria and endoplasmic reticulum during induced apoptosis. Nitric Oxide. **6** (3): 333-41; 2002.

[18] Caputo, M., Bosio, L.A., and Corach, D. Long-term room temperature preservation of corpse soft tissue: an approach for tissue sample storage. Investig Genet. **2**: 17; 2011.

[19] Livak, K.J. and Schmittgen, T.D. Analysis of relative gene expression data using real-time quantitative PCR and the 2(-Delta Delta C(T)) Method. Methods. **25** (4): 402-8; 2001.

[20] Cadenas, E. and Boveris, A. Enhancement of hydrogen peroxide formation by protophores and ionophores in antimycin-supplemented mitochondria. Biochem J. **188** (1): 31-7; 1980.

[21] Boveris, A., Costa, L.E., Cadenas, E., and Poderoso, J.J. Regulation of mitochondrial respiration by adenosine diphosphate, oxygen, and nitric oxide. Methods Enzymol. **301**: 188-98; 1999.

[22] Yonetani, T. Cytochrome oxidase: beef heart. in: Editor^Editors. Methods in Enzymology. 1967: 332-335.

[23] Drew, B. and Leeuwenburgh, C. Method for measuring ATP production in isolated mitochondria: ATP production in brain and liver mitochondria of Fischer-344 rats with age and caloric restriction. Am J Physiol Regul Integr Comp Physiol. **285** (5): R1259-67; 2003.

[24] Navarro, A., Torrejon, R., Bandez, M.J., Lopez-Cepero, J.M., and Boveris, A. Mitochondrial function and mitochondria-induced apoptosis in an overstimulated rat ovarian cycle. Am J Physiol Endocrinol Metab. **289** (6): E1101-9; 2005.

[25] Hickson-Bick, D.L., Jones, C., and Buja, L.M. Stimulation of mitochondrial biogenesis and autophagy by lipopolysaccharide in the neonatal rat cardiomyocyte protects against programmed cell death. J Mol Cell Cardiol. **44** (2): 411-8; 2008.

[26] Lancel, S., Hassoun, S.M., Favory, R., Decoster, B., Motterlini, R., and Neviere, R. Carbon monoxide rescues mice from lethal sepsis by supporting mitochondrial

Accepted manuscript

ACCEPTED MANUSCRIPT

energetic metabolism and activating mitochondrial biogenesis. J Pharmacol Exp Ther. **329** (2): 641-8; 2009.

[27] Suliman, H.B., Carraway, M.S., Welty-Wolf, K.E., Whorton, A.R., and Piantadosi, C.A. Lipopolysaccharide stimulates mitochondrial biogenesis via activation of nuclear respiratory factor-1. J Biol Chem. **278** (42): 41510-8; 2003.

[28] Russell, L.K., Mansfield, C.M., Lehman, J.J., Kovacs, A., Courtois, M., Saffitz, J.E., Medeiros, D.M., Valencik, M.L., McDonald, J.A., and Kelly, D.P. Cardiac-specific induction of the transcriptional coactivator peroxisome proliferator-activated receptor gamma coactivator-1alpha promotes mitochondrial biogenesis and reversible cardiomyopathy in a developmental stage-dependent manner. Circ Res. **94** (4): 525-33; 2004.

[29] Wenz, T. Regulation of mitochondrial biogenesis and PGC-1alpha under cellular stress. Mitochondrion. **13** (2): 134-42; 2013.

[30] Gonzalez, A.S., Elguero, M.E., Finocchietto, P., Holod, S., Romorini, L., Miriuka, S.G., Peralta, J.G., Poderoso, J.J., and Carreras, M.C. Abnormal mitochondrial fusion-fission balance contributes to the progression of experimental sepsis. Free Radic Res. **48** (7): 769-83; 2014.

[31] Nemoto, S., Vallejo, J.G., Knuefermann, P., Misra, A., Defreitas, G., Carabello, B.A., and Mann, D.L. Escherichia coli LPS-induced LV dysfunction: role of toll-like receptor-4 in the adult heart. Am J Physiol Heart Circ Physiol. **282** (6): H2316-23; 2002.

[32] Bonnard, C., Durand, A., Peyrol, S., Chanseaume, E., Chauvin, M.A., Morio, B., Vidal, H., and Rieusset, J. Mitochondrial dysfunction results from oxidative stress in the skeletal muscle of diet-induced insulin-resistant mice. J Clin Invest. **118** (2): 789-800; 2008.

[33] Alvarez, S. and Boveris, A. Mitochondrial nitric oxide metabolism in rat muscle during endotoxemia. Free Radic Biol Med. **37** (9): 1472-8; 2004.

[34] Matsuno, K., Iwata, K., Matsumoto, M., Katsuyama, M., Cui, W., Murata, A., Nakamura, H., Ibi, M., Ikami, K., Zhang, J., Matoba, S., Jin, D., Takai, S., Matsubara, H., Matsuda, N., and Yabe-Nishimura, C. NOX1/NADPH oxidase is involved in endotoxin-induced cardiomyocyte apoptosis. Free Radic Biol Med. **53** (9): 1718-28; 2012.

[35] Beckman, J.S., Beckman, T.W., Chen, J., Marshall, P.A., and Freeman, B.A. Apparent hydroxyl radical production by peroxynitrite: implications for endothelial injury from nitric oxide and superoxide. Proc Natl Acad Sci U S A. **87** (4): 1620-4; 1990.

[36] Stadler, K., Bonini, M.G., Dallas, S., Jiang, J., Radi, R., Mason, R.P., and Kadiiska, M.B. Involvement of inducible nitric oxide synthase in hydroxyl radical-mediated lipid peroxidation in streptozotocin-induced diabetes. Free Radic Biol Med. **45** (6): 866-74; 2008.

[37] Wu, Z., Puigserver, P., and Spiegelman, B.M. Transcriptional activation of adipogenesis. Curr Opin Cell Biol. **11** (6): 689-94; 1999.

[38] Piantadosi, C.A. and Suliman, H.B. Redox regulation of mitochondrial biogenesis. Free Radic Biol Med. **53** (11): 2043-53; 2012.

[39] Milei, J., Grana, D.R., Forcada, P., and Ambrosio, G. Mitochondrial oxidative and structural damage in ischemia-reperfusion in human myocardium. Current knowledge and future directions. Front Biosci. **12**: 1124-30; 2007.

[40] Nakada, K., Inoue, K., and Hayashi, J. Interaction theory of mammalian mitochondria. Biochem Biophys Res Commun. **288** (4): 743-6; 2001.

Accepted manuscript

ACCEPTED MANUSCRIPT

[41] Suliman, H.B., Welty-Wolf, K.E., Carraway, M., Tatro, L., and Piantadosi, C.A. Lipopolysaccharide induces oxidative cardiac mitochondrial damage and biogenesis. Cardiovasc Res. **64** (2): 279-88; 2004.

[42] Chen, C., Deng, M., Sun, Q., Loughran, P., Billiar, T.R., and Scott, M.J. Lipopolysaccharide stimulates p62-dependent autophagy-like aggregate clearance in hepatocytes. Biomed Res Int. **2014**: 267350; 2014.

[43] Fujita, K. and Srinivasula, S.M. TLR4-mediated autophagy in macrophages is a p62-dependent type of selective autophagy of aggresome-like induced structures (ALIS). Autophagy. **7** (5): 552-4; 2011.

[44] Hill, B.G., Benavides, G.A., Lancaster, J.R., Jr., Ballinger, S., Dell'Italia, L., Jianhua, Z., and Darley-Usmar, V.M. Integration of cellular bioenergetics with mitochondrial quality control and autophagy. Biol Chem. **393** (12): 1485-1512; 2012.

[45] Yuan, H., Perry, C.N., Huang, C., Iwai-Kanai, E., Carreira, R.S., Glembotski, C.C., and Gottlieb, R.A. LPS-induced autophagy is mediated by oxidative signaling in cardiomyocytes and is associated with cytoprotection. Am J Physiol Heart Circ Physiol. **296** (2): H470-9; 2009.

FIGURE LEGENDS

Figure 1. Body temperature in control and LPS-treated animals.

* $p < 0.05$ as compared with control group by ANOVA-Dunnett test.

† $p < 0.01$ as compared with control group, ANOVA-Dunnett test.

Figure 2. NO determination in blood as NO-Hb adduct 77 K. **A:** Typical blood EPR spectra; control rats (a), 9 h after LPS-treatment (b) and 12 h after LPS-treatment (c). **B:** NO-Hb signal quantification in control ( ) and LPS-treated animals (•). NO-Hb EPR signal intensities (g = 2.033) were calculated by computer-aided double integration.

Figure 3. PGC-1α **(A)** and mtTFA **(B)** protein expression of left-ventricle myocardium homogenate from control and LPS-treated animals. Panel **(i)** shows typical examples of western blots of cardiac homogenates samples. ß-actin was used as loading control. Bars in panel (**ii**) figure represent densitometric analysis of PGC-1α/ ß-actin ratio or mtTFA/ß-actin ratio blots measurements.

* $p< 0.05$ as compared with control group, ANOVA-Dunnett test.

Figure 4. Cardiac mitochondrial DNA comparative quantification respect nuclear DNA measured by real-time PCR and calculated by the quantification algorithm $2^{-\Delta\Delta Ct}$, for the

ACCEPTED MANUSCRIPT

different time points analyzed. Primers amplifying NADH dehydrogenase 1 gene (mt-Nd1) for mtDNA and Topoisomerase 1 gene (Top1) for nuclear DNA, were used (see Table 1).
* $p < 0.05$ as compared with control group, ANOVA Dunnett test.

Figure 5. p62 **(A)** and LC3 **(B)** protein expression of left-ventricle myocardium homogenate from control and LPS-treated animals. Panel **(i)** shows typical examples of western blots of cardiac homogenates samples. ß-actin was used as loading control. Bars in panel (**ii**) figure represent densitometric analysis of p62/ ß-actin ratio or LC3-II/ß-actin ratio blots measurements.
* $p< 0.05$ as compared with control group, ANOVA-Dunnett test.
† $p< 0.01$ as compared with control group, ANOVA-Dunnett test.
$^{\&}$ $p< 0.01$ as compared with LPS group (6h), ANOVA-Bonferroni test.

Figure 6. Representative transmission electron micrographs of left-ventricle myocardium from control (A, B), LPS 6h (C-F), LPS 18h (G-I) and LPS 24h (J, K) animals. **A**, **B**: control animals displayed normal mitochondria morphology. Typical organization of mitochondria clearly displayed the internal membrane (im) comprising cristae and well defined mitochondrial outer membrane (om). **C-F**: 6 h after LPS administration, mitochondria displayed several abnormalities, such as formation of internal vesicles (**C**), loss and/or disruption of cristae, clearer matrix and swelling (black arrows, in D and F). **G-I**: 18 h after LPS administration, mitochondria displayed degenerative changes including swelling (sm, black arrows) and internal vacuoles associated with mitochondrial membranes (vmm, black arrows). **J-K**: 24h after LPS administration mitochondria with fusion/fission associated morphology (arrow), inner membrane disruption were observed (* in K). Also mitochondria of irregular size were observed. Scale bars: 0.4 µm in **A**, 0.2 µm in **B**, 1 µm in **C**, E and **G**, 400 nm in **D** and **F**, 0.5 µm in **H** and I, 0.6 µm, 0.6 µm in **J** and **K**.

Figure 7. Representative traces obtained during the measurements of heart mitochondrial O_2 consumption. The traces show state 4 and state 3 respiration rates for control mitochondria and 6-24 h after LPS challenge.

Figure 8. ATP production rate in left-ventricle myocardium mitochondria from control and LPS-treated rats. Malate plus glutamate were used as substrates.
* $p < 0.05$ as compared with control group, ANOVA Dunnett test.

Accepted manuscript

ACCEPTED MANUSCRIPT

Table 1 Primers for quantitative PCR (qPCR).

	Forward (sequence)	**Reverse** (sequence)
Top 1	3´-GGCTGGTTTGGTCTACCTGA-5´	3´-TCATTGGATGAATCGAGGAA-5´
Mt-Nd1	3´-CCTCACCCCCTTATCAACCT-5´	3´-GTAAGAGATGGTTTGGGCAAC-5´

Table 2 Cardiac cytochrome oxidase activity, as a marker of mitochondrial mass, in control and LPS-treated animals.

	Cytochrome oxidase activity		**Activity ratio**
	homogenate	**mitochondria**	**homogenate/mitochondria**
	k'_1 (min^{-1})/g tissue	k'_2 (min^{-1})/mg protein	k'_1/k'_2(mg protein/g tissue)
Control	497±8	46.8±1.6	10.7±0.5
LPS 6h	407±32	41.5±1.5	9.7±0.5
LPS 9h	604±61	60.1±3.7‡	10.0±0.7
LPS 12h	486±33	50.1±3.4	9.7±0.5
LPS 18h	526±24	46.1±1.3	11.4±0.5
LPS 24h	517±31	39.1±1.8*	13.9±1.2*

*p<0.05 as compared to control group by ANOVA-Dunnett test, n=5.
†p<0.01 as compared to control group by ANOVA-Dunnett test, n=5.

Table 3 Cardiac mitochondrial density and ultrastructure in control and LPS-treated animals.

	Mitochondrial density ($\mu m^3/\mu m^3$ total)	**Damaged mitochondria** (%)
Control	0.330±0.024	1.4±0.3
LPS 6 h	0.391±0.028*	6.3±1.7‡
LPS 18 h	0.308±0.024	3.6±1.6
LPS 24 h	0.315±0.025	4.3±1.3

*p<0.01 as compared to control group by ANOVA-Dunnett test, n=5.
†p<0.05 as compared to control group by ANOVA-Dunnett test, n=5.

Table 4 Cardiac mitochondria respiration in control and LPS-treated animals.

O_2 consumption (ng-at O/min.mg protein)		
	Malate+Glutamate	**Succinate**

Accepted manuscript

ACCEPTED MANUSCRIPT

	state 4	state 3	RCR	state 4	state 3	RCR
Control	29.4±3.2	226±15	7.7±0.2	59.7±6.2	159±5	2.66±0.10
LPS 6h	25.5±2.0	181±9*	7.1±0.1*	55.6±3.1	146±8	2.63±0.08
LPS 18 h	29.6±2.0	173±4‡	5.6±0.1‡	61.7±2.5	144±10	2.33±0.09*
LPS 24 h	28.0±2.1	170±10‡	6.1±0.1‡	56.7±1.3	130±6*	2.29±0.06‡

*p<0.05 with respect to control group by ANOVA-Dunnett test, n=5.
†p<0.1 with respect to control group by ANOVA-Dunnett test, n=5.

Table 5 Cardiac mitochondrial respiratory chain complexes (I, II and IV) activity in control and LPS-treated animals.

	complex I	**complex II**	**complex IV**
	nmol/min.mg protein)	(nmol/min.mg protein)	[k'_2 (min^{-1})/mg protein]
Control	328±22	177±10	46.8±1.6
LPS 6 h	234±23*	170±13	41.5±1.5
LPS 18h	235±27*	169±10	46.1±1.3
LPS 24 h	187±23†	122±16*	39.1±1.8*

*p<0.05 as compared to control group by ANOVA-Dunnett test, n=5.
† p<0.01 as compared to control group by ANOVA-Dunnett test, n=5.

Accepted manuscript

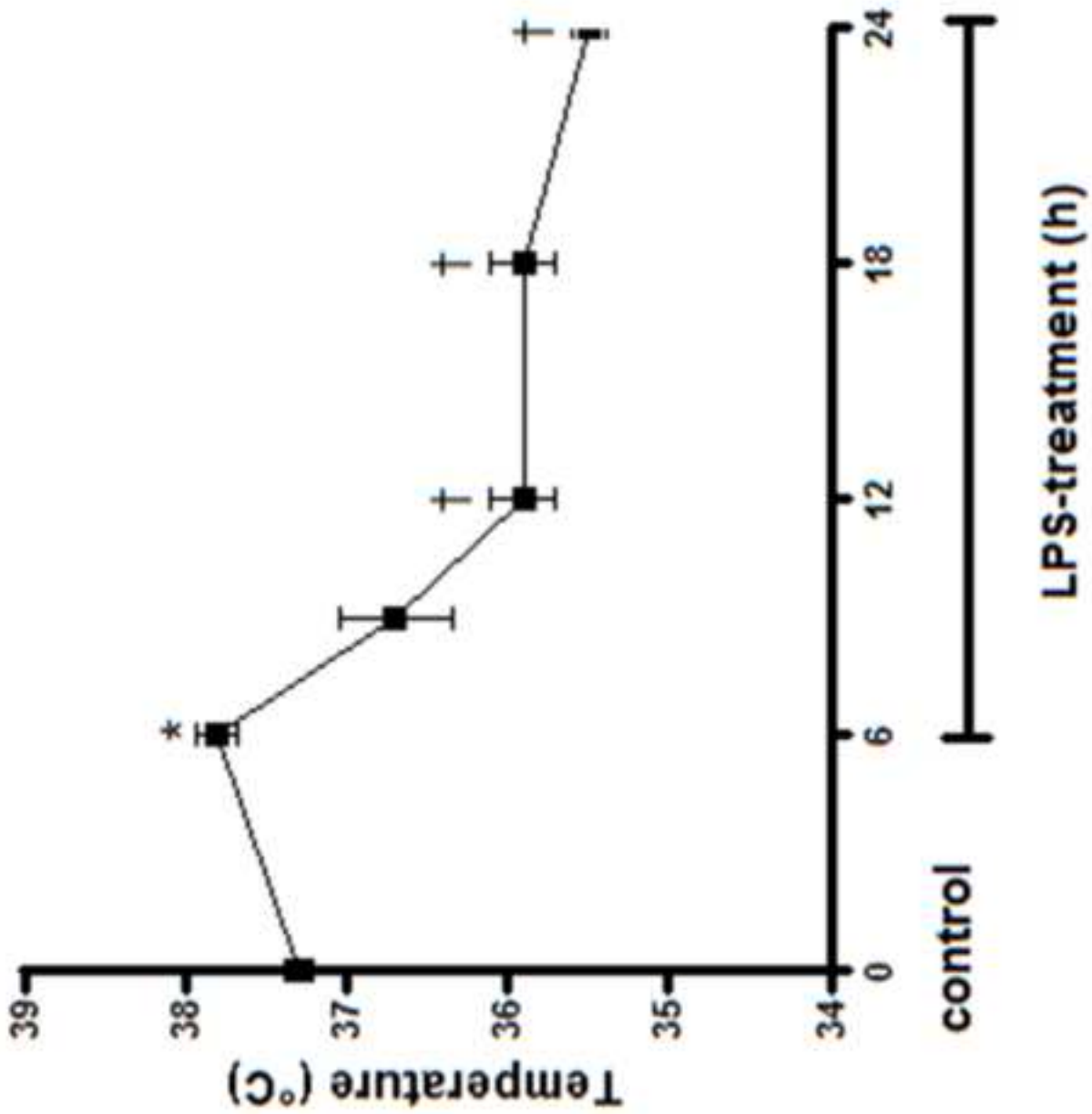
Temperature (°C)
39
38
37
36
35
34
0
6
12
18
24
LPS-treatment (h)
control
*
†
†
†
†

Figure 1

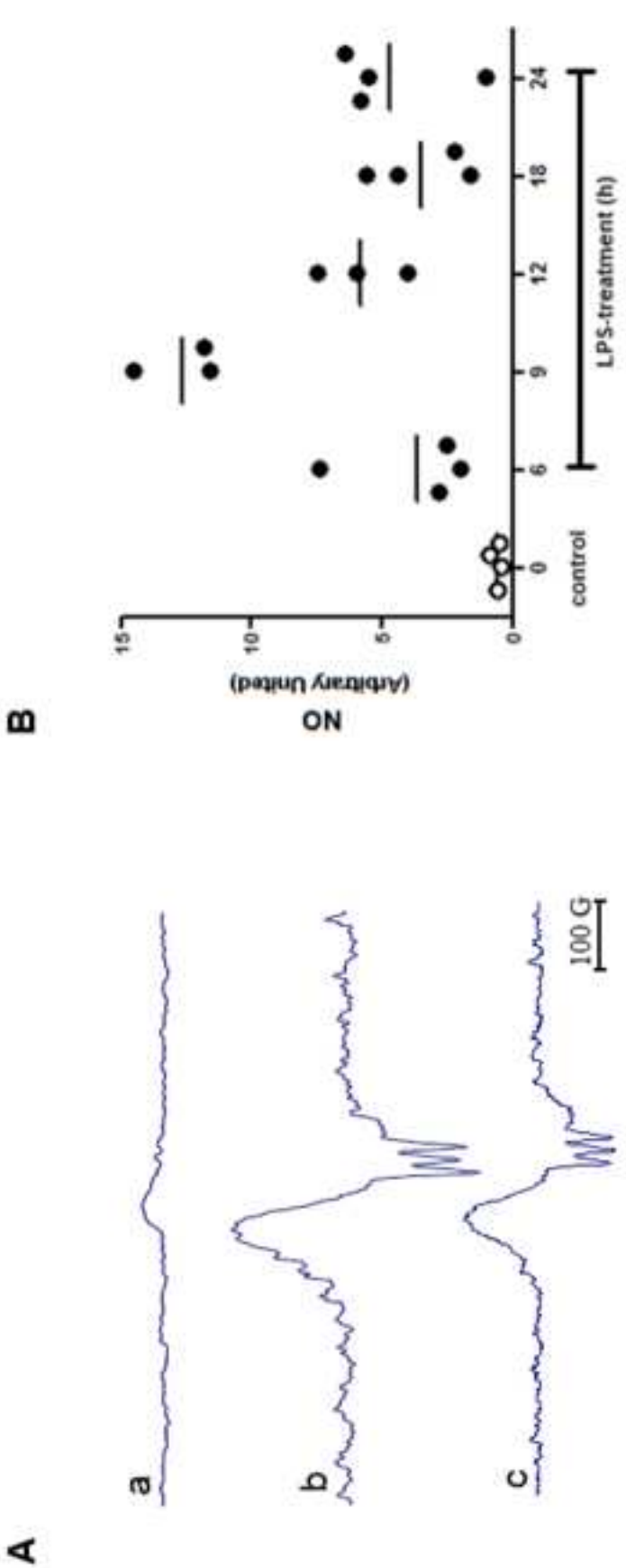
A
a
b
c
100 G
B
NO
(Arbitrary Unites)
15
10
5
0
0
6
9
12
18
24
control
LPS-treatment (h)

Figure 2

Figure 3

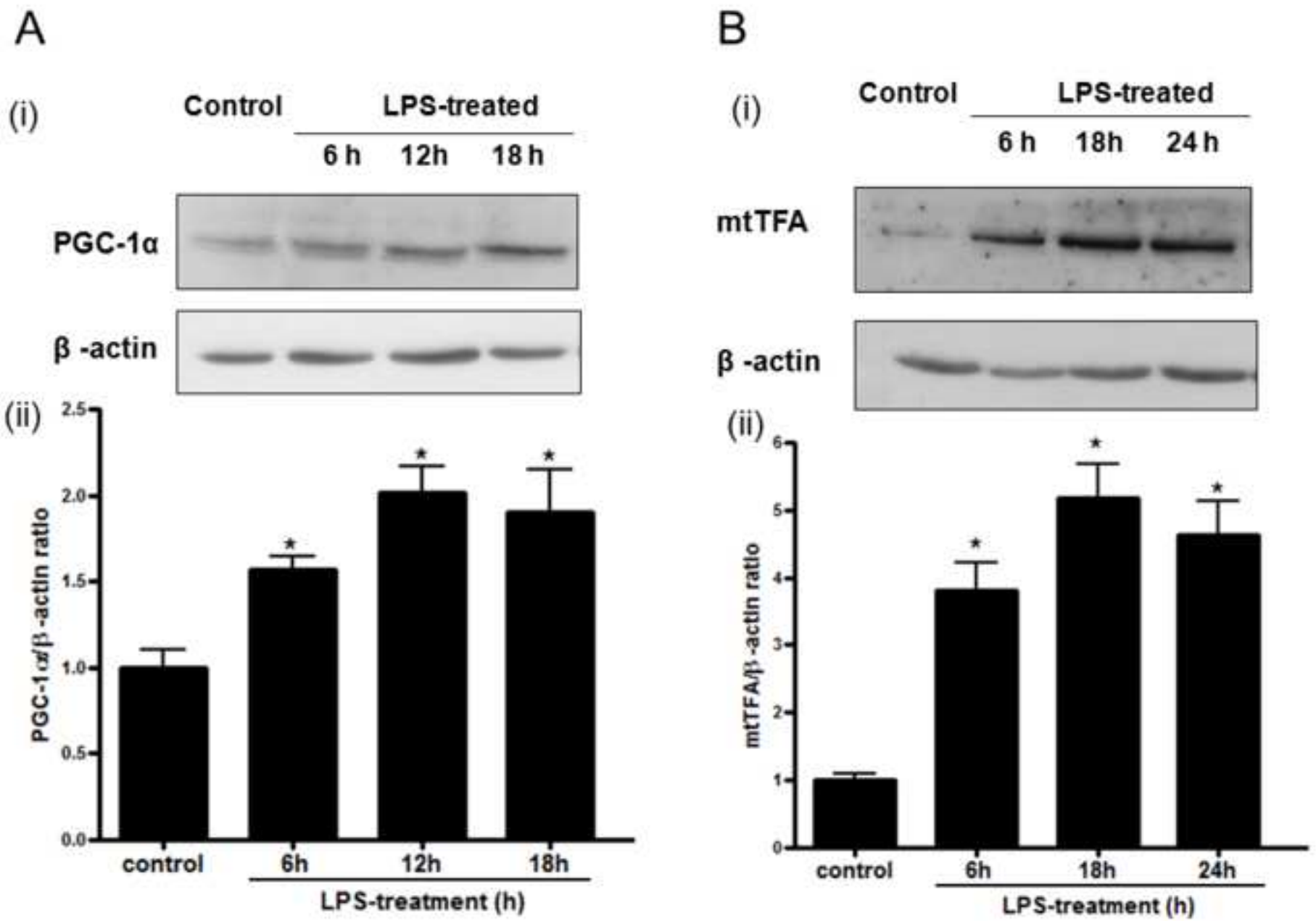

ACCEPTED MANUSCRIPT

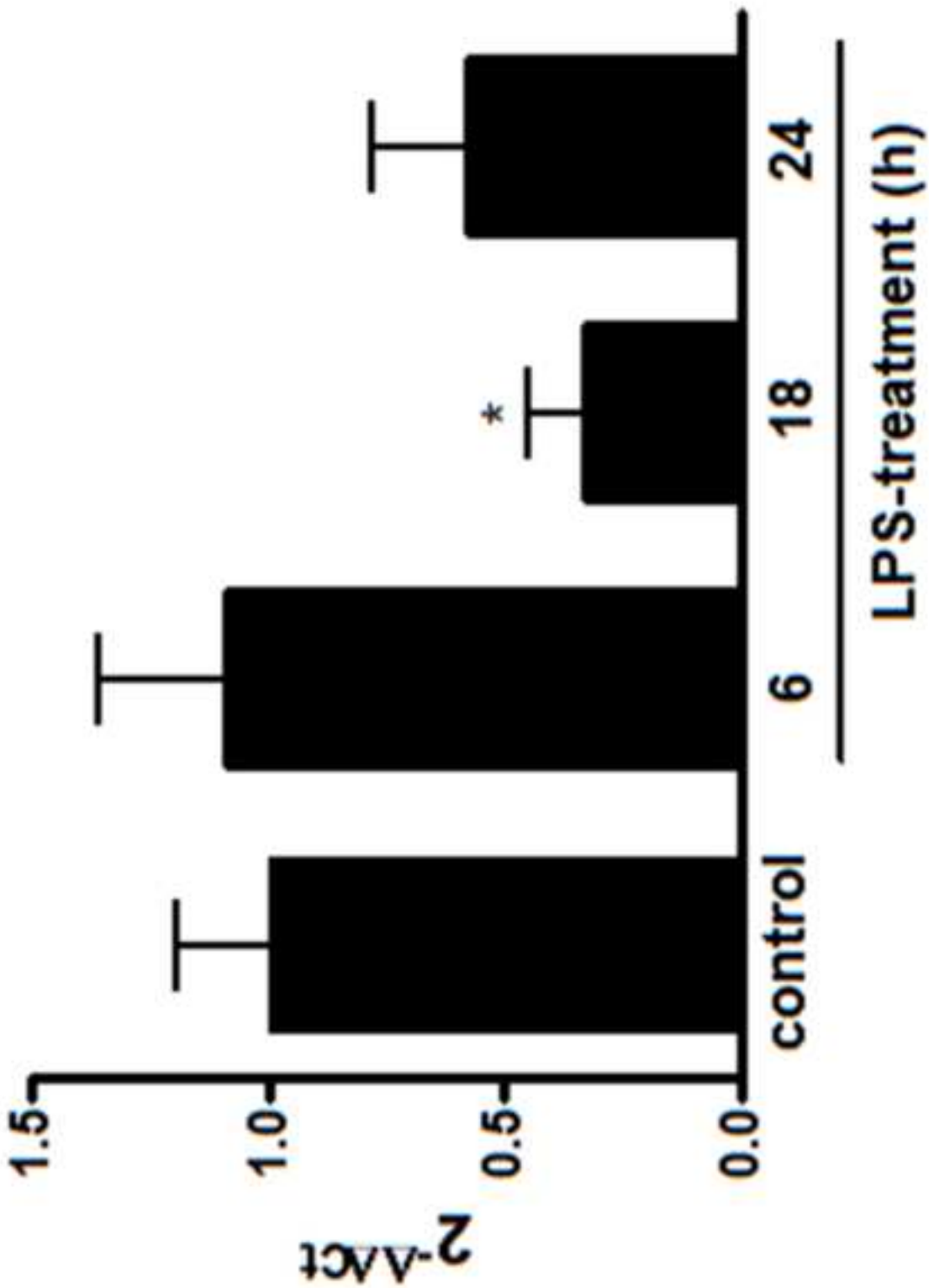

Figure 4

Figure 5

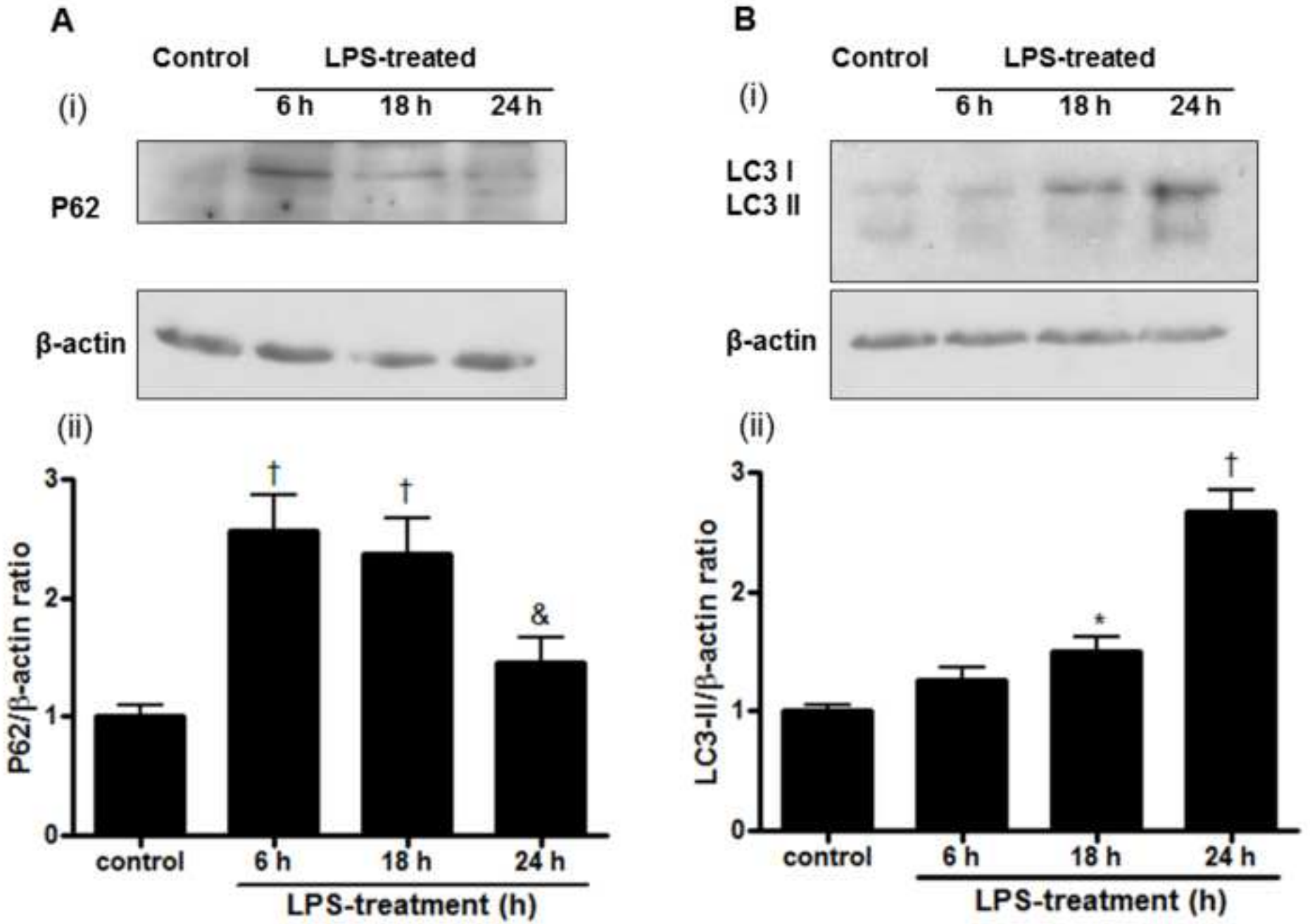

ACCEPTED MANUSCRIPT

Figure 6

ACCEPTED MANUSCRIPT

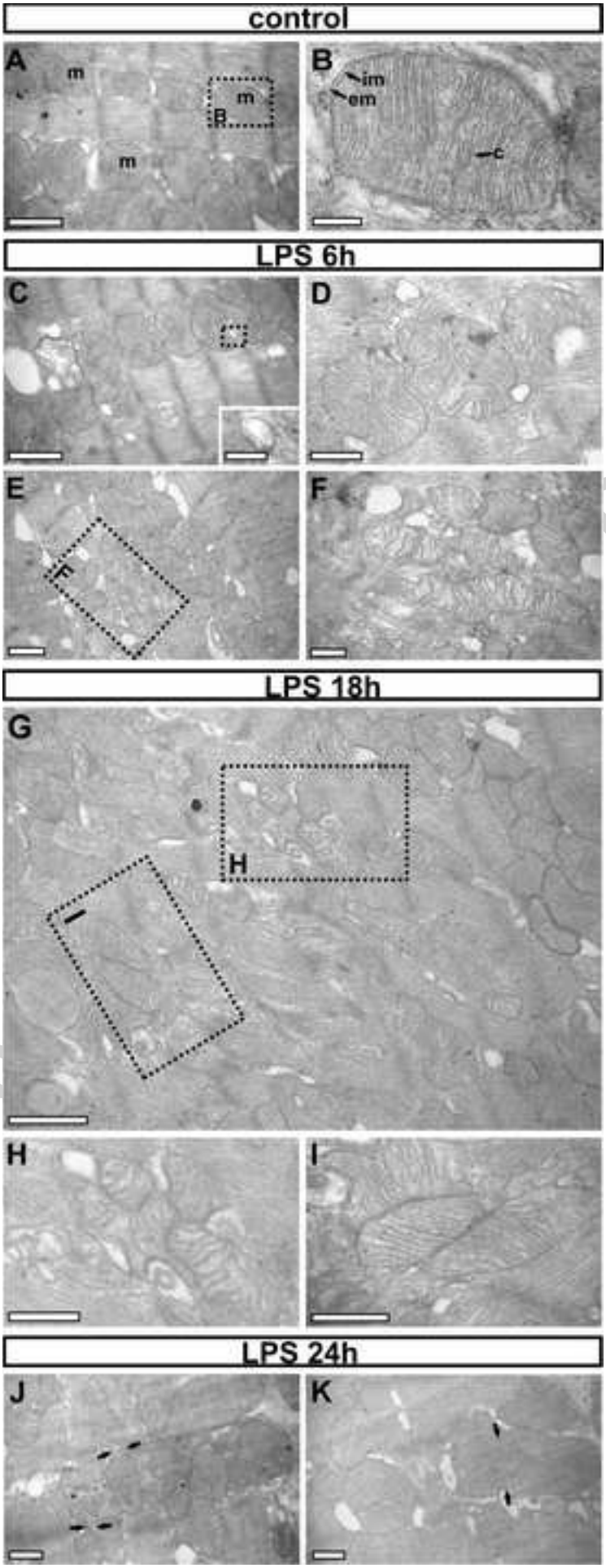

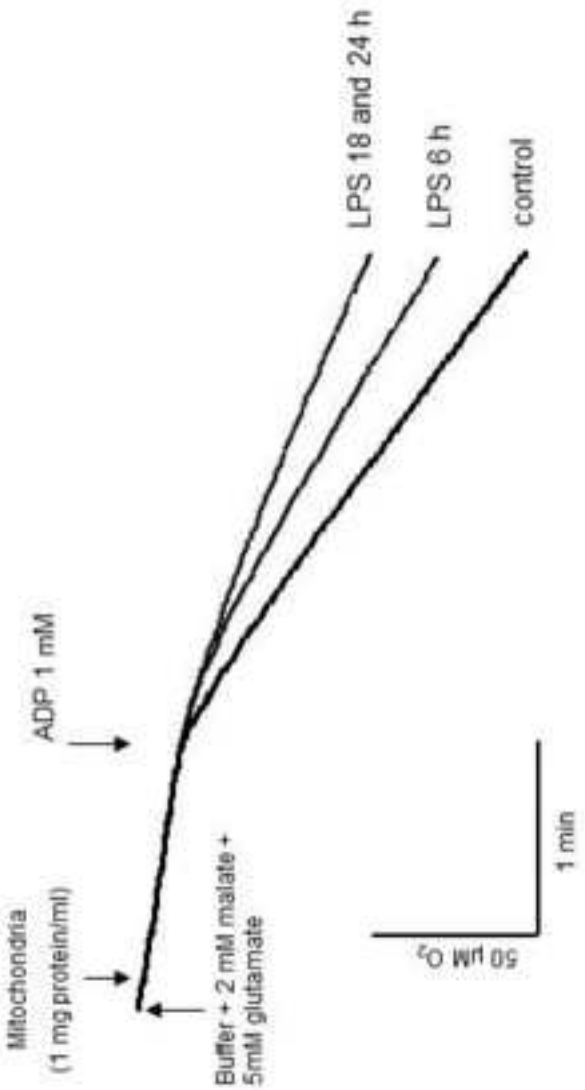
LPS 18 and 24 h
LPS 6 h
control
ADP 1 mM
Mitochondria
(1 mg protein/ml)
Buffer + 2 mM malate +
5mM glutamate
50 µM O2
1 min

Figure 7

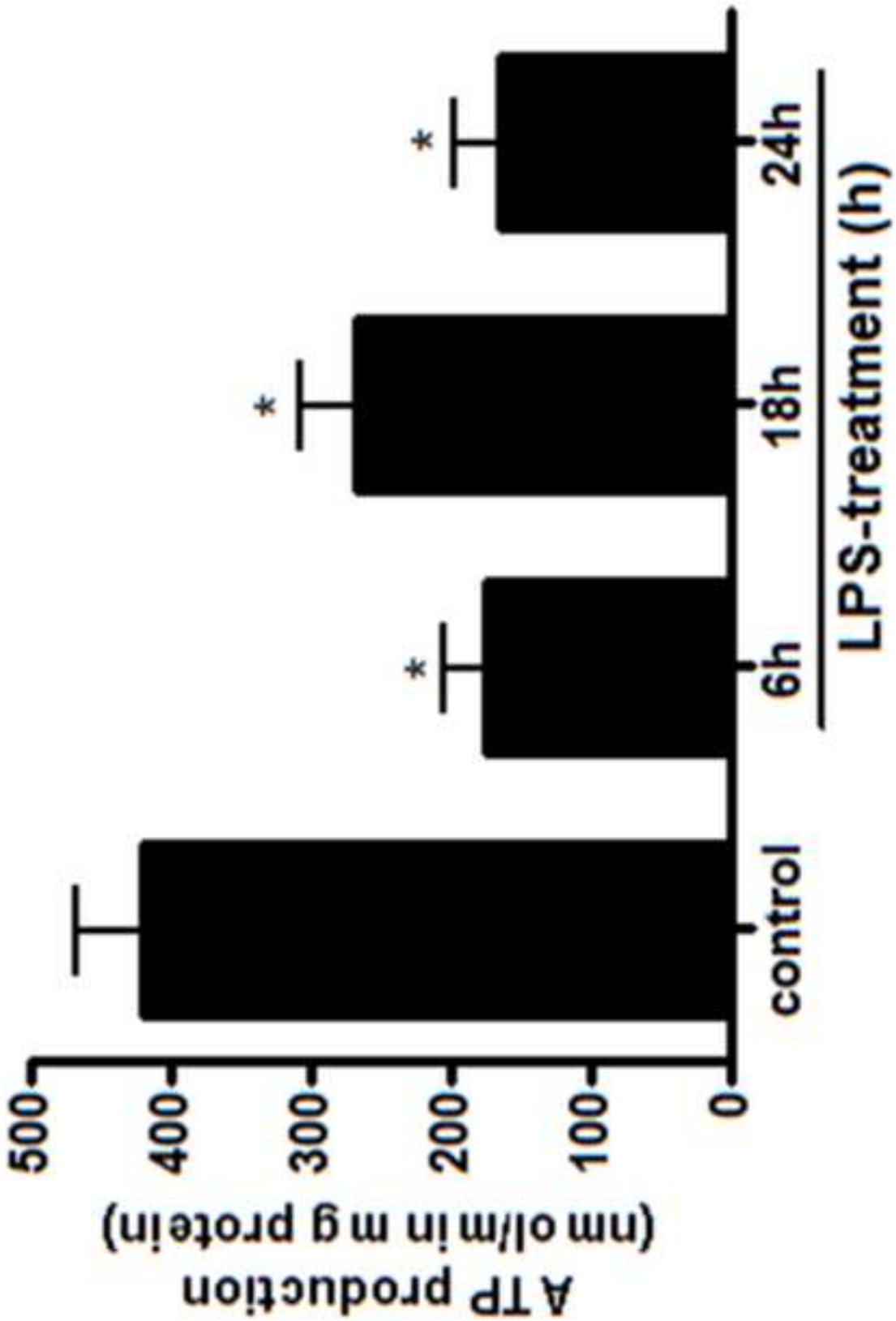
ATP production
(nm ol/m in m g protein)
500
400
300
200
100
0
control
6h
18h
24h
LPS-treatment (h)
*
*
*

Figure 8